# Influence of Rotation on Vibration Behavior of a Functionally Graded Moderately Thick Cylindrical Nanoshell Considering Initial Hoop Tension

H. Safarpour, M.M. Barooti, M. Ghadiri [*]

*Faculty of Engineering, Department of Mechanics, Imam Khomeini International University, Qazvin, Iran*

## ABSTRACT

In this research, the effect of rotation on the free vibration is investigated for the size-dependent cylindrical functionally graded (FG) nanoshell by means of the modified couple stress theory (MCST). MCST is applied to make the design and the analysis of nano actuators and nano sensors more reliable. Here the equations of motion and boundary conditions are derived using minimum potential energy principle and first-order shear deformation theory (FSDT). The formulation consists of the Coriolis, centrifugal and initial hoop tension effects due to the rotation. The accuracy of the presented model is verified with literatures. The novelty of this study is the consideration of the rotation effects along with the satisfaction of various boundary conditions. Generalized differential quadrature method (GDQM) is employed to discretize the equations of motion. Then the investigation has been made into the influence of some factors such as the material length scale parameter, angular velocity, length to radius ratio, FG power index and boundary conditions on the critical speed and natural frequency of the rotating cylindrical FG nanoshell.                © 2019 IAU, Arak Branch.All rights reserved.

Keywords : Critical speed; Initial hoop tension; Functionally graded material; GDQM; Moderately thick cylindrical nanoshell; Modified couple stress theory.

## 1 INTRODUCTION

BECAUSE of simple manufacturing and great strength to weight ratio, use of cylindrical shell structures prevail in many industries. The material of cylindrical shell model has a direct effect on the vibration behaviour. Functionally graded materials (FGMs) are a new group of materials which have many advantages and superior properties, including high temperature resistance and high strength. The cylindrical FG shells can be applied to fuselage structures of civil airliners, aerospace structures, military aircraft propulsion system, and other engineering fields. Ref [1] proposed the Free vibration analysis of cylindrical FG micro/nanoshells structures. The background of dynamic analysis of rotating cylindrical shells is about a hundred years old. Bryan [2] studied rotating cylindrical shell, considering a rotating ring for the first time. He found the traveling mode for the first time. later, Taranto and Lesson [3] made an investigation into the rotating shells with Coriolis effect. Then, Srinivasan and Lauterbach [4]

___
[*]Corresponding author. Tel.: +98 28 33901144; Fax: +98 28 33780084.
*E-mail address: ghadiri@eng.ikiu.ac.ir* (M. Ghadiri).

studied traveling waves of infinite rotating cylindrical shells. Zohar and Aboudi [5] analyzed rotating finite thin cylinder while Padovan [6] began to work on natural frequencies of rotating prestressed cylinder using thin shell theory. In addition, he applied numerical method and finite element method to achieve asymmetric frequencies and buckling loads of anisotropic prestressed cylinder [7, 8]. A decade later, Endo et al.[9] theoretically solved flexural vibration of a cylindrical thin ring, and made comparison with experiment. Saito and Endo [10] repeated their previous problem two years later, considering initial tension. So far only has free vibration of rotating cylinder been analyzed. But Huang and Soedel [11] worked on free and force vibration of a finite cylinder with simply supported boundaries. As the main result, they made a conclusion that rotation forces natural frequencies to bifurcate into two branches as forward and backward waves. Moreover, Huang and Hsu [12] studied the influence of harmonic moving load on the resonant of a rotating cylindrical shell. Rotating cylindrical FG shells have caught on in the recent years because of their promising future to be used in various industries. These rotating nano structures can be used as MEMS gyroscope sensors [13]. Use of these rotating nano structures can reduce cost, size, and weight, MEMS gyroscopes potentially have a wide range of application in the industries such as high performance navigation systems, advanced automotive safety systems, stabilization of image in digital cameras. Gyroscopes built in nano/micro scales open new window to creation of nano/micro-satellites, nano/micro robots, and implants to cure vestibular disorders. In addition, the investigation of their vibration characteristics of rotation cylindrical FG nanoshell is of great interest for engineering design and manufacture [14-16]. The experiments show that the size effects play an important role in mechanical properties. Thus, avoiding these effects may result wrong designs and unacceptable answers. It should be noted that the size effect is not considered in the classical continuum theories,so this theory is not appropriate for micro and nano scales. One of the non-classical theories that consider the effects of size is couple stress theory. Toupin, Koiter, and Mindlin [17-19] investigated the couple stress theory including higher order rotation gradients, which is in fact the asymmetric part of the deformation gradient. According to this theory, it includes four material constants (two classical and two additional) for isotropic elastic materials. As an example of this theory, Asghari et al [20] presented the size effects in Timoshenko beams on the basis of the couple stress theory. it is difficult to determine the microstructure related length scale parameters. Therefore, we are looking for the continuum theory which involves only one additional material parameter of length scale. Modified couple stress theory is one of the best and most well-known continuum mechanics theories that include small scale effects with reasonable accuracy in micro scale devices. Yang et al [21] presented a modified couple stress theory, in which the couple stress tensor is symmetric and only one internal material length scale parameter is involved, unlike the classical couple stress theory mentioned above. Many researchers have used this theory to examine the dynamic and static behavior of micro-beams, micro-plates and micro-shells [22-25]. It is noted that , nonlocal theory of Eringen is one of the best and most well-known continuum mechanics theories that includes small scale effects with good accuracy in nano/micro scale devices, but the results show that modified couple stress theory coincides with experimental results better than Eringen's nonlocal elasticity and classical theories [26]. Therefore, in this study, the modified couple stress theory has been used. There are a lot of theories which are used for analysis of cylindrical shell. The first one is Love classical theory [27] that is presented for analysis of thin plates and shells. After that, many researchers such as Donnell [28], Sanders [29] and others combined their geometrical assumptions with classical linear elasticity theory and introduced their theories. Leissa investigated a good collection for these theories and their application [30]. These theories of shell have been based on some assumptions. In the theories of classical shell, it is assumed that the stresses are constant within the thickness. Consequently, because of this assumption the theories of classical shell cannot present precise result for thick and moderately thick shells. First order shear deformation theory (FSDT) was presented by Reissner [31] and Mindlin [32] to compensate the defects of the classical theory. Ghorbanpour Arani et al [33] studied nonlinear vibration of double-walled carbon nanotube (DWCNT) embedded in an elastic medium and subjected to an axial fluid flow. In another work, Ghorbanpour Arani et al [34] presented nonlinear vibration and instability of embedded double-walled boron nitride nanotubes based on nonlocal cylindrical shell theory. Recently Hashemi et al [35] investigated free vibrations of spinning nanotube based on nonlocal first order shear deformation shell theory using exact solution. It should be noted that the previous studies have not taken into account the size effect and initial hoop tension on a rotary cylindrical FG nanoshell while they were using MCST. The novelty of current study is consideration of the rotation, initial hoop tension and size effect as well as satisfying various boundary conditions implemented on the cylindrical FG nanoshell while using MCST. Generalized differential quadrature method (GDQM) is employed to solve the governing equation with every kind of boundary condition because of its efficiency and high accuracy. FG cylinders normally are modeled and analysed along their thickness while the outer surface is metal and the inner surface is ceramic.

For the first time, present study considers the size dependency of the transverse vibration of a rotary cylindrical FG nanoshell, using modified couple stress theory. The governing equations and boundary conditions have been

developed using Hamilton principle and are solved with the aid of the GDQM. The results show that, material length scale parameter, angular velocity, length to radius ratio, FG power index and boundary conditions play important roles on the natural frequency of rotating cylindrical FG nanoshell.

## 2   POWER –LOW FG NANOSHELL EQUATIONS BASE

To have better understanding of the importance and applications of the proposed model, Fig. 1 demonstrates a rotating cylindrical nanoshell which can turn salt water into fresh water [36]. In addition, Fig. 2 shows a rotating FG cylindrical nanoshell, where $x$, $\theta$, and $z$ denote the orthogonal curvilinear coordinates on the middle surface ($z = 0$). The thickness, length, and the middle surface radius of cylindrical shell are denoted by $h$, $L$, and $R$ respectively. At the inner and the outer surfaces, the functionally graded nanoshell is generally composed of two different materials. The FG cylindrical nanoshell is made of porous material and according to the power law distribution, its bulk elastic modulus $E(z)$, mass density $\rho(z)$, and Poisson's ratio $v(z)$ are assumed to change along the thickness direction [37]. Power FG index ($N$) determines the variation profile of material properties across the cylindrical FG nanoshell thickness. Assuming that the inner surface is ceramic and the outer surface is metal, then for different values of $N$, the mechanical properties can be written as:

$$E(\hat{z}) = (E_m - E_c)(\frac{\hat{z}}{h})^N + E_c - (E_c + E_m)\frac{\alpha}{2}$$

$$\rho(\hat{z}) = (\rho_m - \rho_c)(\frac{\hat{z}}{h})^N + \rho_c - (\rho_c + \rho_m)\frac{\alpha}{2} \qquad (1)$$

$$v(\hat{z}) = (v_m - v_c)(\frac{\hat{z}}{h})^N + v_c - (v_c + v_m)\frac{\alpha}{2}$$

In Eq.(1) $\hat{z}$ stands for the distance of arbitrary surface from the inner ones of the cylindrical shell.
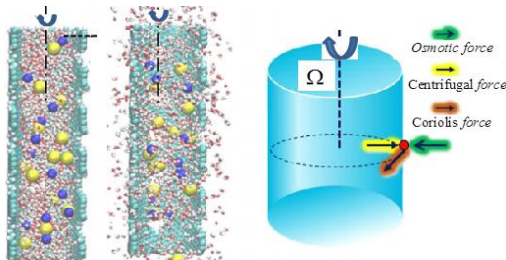


**Fig.1**
One applications of the rotating cylindrical nanoshell model [36].
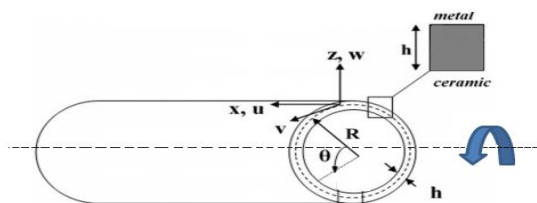


**Fig.2**
Geometry of the rotating cylindrical FG nanoshell.

*2.1 Modified couple stress theory*

Yang et al.[21] presented modified couple stress theory for the first time. According to this theory, the strain energy expressed as a function of rotation tensor gradient and strain tensor, in addition, it includes one length scale parameter and two Lame parameters. According to this theory, the strain energy is expressed as:

$$U = \frac{1}{2}\iiint_V (\sigma_{ij}\varepsilon_{ij} + m_{ij}^s \chi_{ij}^s)dV \qquad (2)$$

In Eq. (2), $\chi_{ij}^s$, $\varepsilon_{ij}$, $\sigma_{ij}$ and $m_{ij}^s$ respectively represent the components of symmetric rotation gradient tensor, strain tensor, stress tensor, and higher order stress tensor, which are expressed as:

$$\varepsilon_{ij} = \frac{1}{2}(u_{i,j} + u_{j,i})\tag{3}$$

$$\chi_{ij}^s = \frac{1}{2}(\varphi_{i,j} + \varphi_{j,i})\tag{4}$$

$$m_{ij}^s = 2l^2\mu(\hat{z})\chi_{ij}^s, \quad \varphi_i = \frac{1}{2}[curl(u)]_i\tag{5}$$

where $u_i$ and $\phi_i$ respectively represent the component of displacement vector, and infinitesimal rotation vector. In Eq. (5), $l$ is the parameter which denotes the additional independent material length-scale parameter that is related to the symmetric rotation gradients. Note that, the length scale parameter is assumed constant in FG cylindrical shell. In addition, the stress–strain relation can be expressed as follows:

$$\begin{Bmatrix} \sigma_{xx} \\ \sigma_{\theta\theta} \\ \sigma_{x\theta} \\ \sigma_{\theta z} \\ \sigma_{xz} \end{Bmatrix} = \begin{bmatrix} C_{11} & C_{12} & 0 & 0 & 0 \\ C_{12} & C_{22} & 0 & 0 & 0 \\ 0 & 0 & C_{66} & 0 & 0 \\ 0 & 0 & 0 & C_{44} & 0 \\ 0 & 0 & 0 & 0 & C_{55} \end{bmatrix} \begin{Bmatrix} \varepsilon_{xx} \\ \varepsilon_{\theta\theta} \\ 2\varepsilon_{x\theta} \\ 2\varepsilon_{\theta z} \\ 2\varepsilon_{xz} \end{Bmatrix}\tag{6}$$

where $C_{ij}$ is the elasticity matrix component. The stiffness coefficients are expressed as:

$$C_{11} = \frac{E(\hat{z})}{1 - v(\hat{z})^2}, \; C_{12} = v(\hat{z})C_{11}, \; C_{22} = C_{11}, \; C_{44} = C_{55} = C_{66} = \frac{E(\hat{z})}{2(1 + v(\hat{z}))}\tag{7}$$

*2.2 Displacement field of cylindrical shell*

According to first order shear deformation theory, the displacement field of cylindrical FG nanoshell along the three directions of $x$, $\theta$, and $z$ is expressed as [38]:

$$\begin{aligned} U(x,\theta,z,t) &= u(x,\theta,t) + z\psi_x(x,\theta,t) \\ V(x,\theta,z,t) &= v(x,\theta,t) + z\psi_\theta(x,\theta,t) \\ W(x,\theta,z,t) &= w(x,\theta,t) \end{aligned}\tag{8}$$

In Eq. (8), $u(x,\theta,t)$, $v(x,\theta,t)$, and $w(x,\theta,t)$ are considered as neutral axis displacement, and $\psi_\theta(x,\theta,t)$ and $\psi_x(x,\theta,t)$ as rotation of a transverse normal surface about the circumferential and axial directions. the position of the neutral axis is given by [39]:

$$\int_A \sigma_{xx}dA = \int_A \frac{E(\hat{z})}{1 - v^2(\hat{z})}\left(z\frac{\partial^2 w}{\partial x^2}\right)dA = 0\tag{9}$$

where

$$z = \hat{z} - \hat{z}_c\tag{10}$$

By substituting Eq.(10) in (9) ,

$$\hat{z}_c = \frac{\int_A \frac{E(\hat{z})}{1-v^2(\hat{z})}\hat{z}\,dA}{\int_A \frac{E(\hat{z})}{1-v^2(\hat{z})}dA}$$

(11)

### 2.3 Governing equations and boundary conditions

To derive equations of motion and boundary conditions for functionally graded cylindrical shell, using the modified couple stress theory and first order shear deformation shell model, one must insert the components of the displacement field into the strains. Now by substituting the Eq.(8) into Eq.(3), Eq.(4) and Eq.(5), the components of the deviatoric stretch gradient tensor and the strain tensor obtains as follows [38]:

$$\varepsilon_{xx} = \frac{\partial u}{\partial x} + z\frac{\partial \psi_x}{\partial x}$$
$$\varepsilon_{\theta\theta} = \frac{1}{R}\frac{\partial v}{\partial \theta} + z\frac{1}{R}\frac{\partial \psi_\theta}{\partial \theta} + \frac{w}{R}$$
$$\varepsilon_{xz} = \frac{1}{2}(\psi_x + \frac{\partial w}{\partial x})$$
$$\varepsilon_{x\theta} = \frac{1}{2}(\frac{1}{R}\frac{\partial u}{\partial \theta} + \frac{\partial v}{\partial x}) + \frac{z}{2}(\frac{1}{R}\frac{\partial \psi_x}{\partial \theta} + \frac{\partial \psi_\theta}{\partial x})$$
$$\varepsilon_{\theta z} = \frac{1}{2}(\psi_\theta + \frac{1}{R}\frac{\partial w}{\partial \theta} - \frac{v}{R})$$

(12)

Moreover, the non-zero components of symmetric rotation gradient tensor obtain as follows:

$$\chi^s_{xx} = -\frac{1}{2}(\frac{\partial \psi_\theta}{\partial x} + \frac{1}{R}\frac{\partial v}{\partial x} - \frac{1}{R}\frac{\partial^2 w}{\partial x\,\partial \theta})$$
$$\chi^s_{\theta\theta} = -\frac{1}{2R}(\frac{1}{R}\frac{\partial u}{\partial \theta} - \frac{\partial v}{\partial x} - z\frac{\partial \psi_\theta}{\partial x}) - \frac{1}{2}(\frac{1}{R}\frac{\partial^2 w}{\partial x\,\partial \theta} - \frac{1}{R}\frac{\partial \psi_x}{\partial \theta})$$
$$\chi^s_{zz} = -\frac{1}{2}(\frac{1}{R}\frac{\partial \psi_x}{\partial \theta} - \frac{\partial \psi_\theta}{\partial x} - \frac{1}{R^2}\frac{\partial u}{\partial \theta})$$
$$\chi^s_{x\theta} = -\frac{1}{4}(\frac{1}{R^2}\frac{\partial v}{\partial \theta} + \frac{\partial^2 w}{\partial x^2} - \frac{1}{R^2}\frac{\partial^2 w}{\partial \theta^2} - \frac{\partial \psi_x}{\partial x} + \frac{1}{R}\frac{\partial \psi_\theta}{\partial \theta})$$
$$\chi^s_{xz} = -\frac{1}{4}(\frac{1}{R}\frac{\partial^2 u}{\partial x\,\partial \theta} - \frac{\partial^2 v}{\partial x^2} - \frac{v}{R^2} + \frac{1}{R^2}\frac{\partial w}{\partial \theta} + \frac{\psi_\theta}{R}) - \frac{z}{4}(\frac{1}{R}\frac{\partial^2 \psi_\theta}{\partial x\,\partial \theta} - \frac{\partial^2 \psi_\theta}{\partial x^2})$$
$$\chi^s_{\theta z} = -\frac{1}{4}(\frac{1}{R^2}\frac{\partial^2 u}{\partial \theta^2} - \frac{1}{R}\frac{\partial^2 v}{\partial x\,\partial \theta} - \frac{1}{R}\frac{\partial w}{\partial x} + \frac{\psi_x}{R}) - \frac{z}{4}(\frac{1}{R^2}\frac{\partial^2 \psi_x}{\partial \theta^2} - \frac{1}{R}\frac{\partial^2 \psi_\theta}{\partial x\,\partial \theta})$$

(13)

For the equations of the motion and boundary conditions, the principle of minimum potential energy states that [40]:

$$\int_{t_1}^{t_2}(\delta T - \delta U - \delta U_h)dt = 0$$

(14)

In Eq. (14) $\delta T$ , $\delta U$ and $\delta U_h$ respectively represent the first variation of kinetic energy, strain energy and potential energy. Strain energy of cylindrical FG nanoshell based on modified couple stress theory is expressed as follows:

$$\delta U = \frac{1}{2}\iiint_V (\sigma_{ij}\delta\varepsilon_{ij} + m_{ij}^s\delta\chi_{ij}^s)dV = \delta U_1 + \delta U_2$$

$$\delta U_1 = \frac{1}{2}\iiint_V (\sigma_{ij}\delta\varepsilon_{ij})dV = \iint_A \left\{ \begin{array}{l} (N_{xx}\frac{\partial}{\partial x}\delta u + M_{xx}\frac{\partial}{\partial x}\delta\psi_x) + N_{\theta\theta}(\frac{1}{R}\frac{\partial}{\partial\theta}\delta v + \frac{\delta w}{R}) + \\[2mm] M_{\theta\theta}\frac{1}{R}\frac{\partial}{\partial\theta}\delta\psi_\theta + Q_{xz}(\delta\psi_x + \frac{\partial}{\partial x}\delta w) + \\[2mm] N_{x\theta}(\frac{1}{R}\frac{\partial}{\partial\theta}\delta u + \frac{\partial}{\partial x}\delta v) + M_{x\theta}(\frac{1}{R}\frac{\partial}{\partial\theta}\delta\psi_x + \frac{\partial}{\partial x}\delta\psi_\theta) \\[2mm] + Q_{z\theta}(\delta\psi_\theta + \frac{1}{R}\frac{\partial}{\partial\theta}\delta w - \frac{\delta v}{R}) \end{array} \right\} Rdxd\theta$$

$$\delta U_2 = \frac{1}{2}\iiint_V (m_{ij}^s\delta\chi_{ij}^s)dV = \iint_A \left\{ \begin{array}{l} (-\frac{Y_{\theta\theta}}{2R^2} + \frac{Y_{zz}}{2R^2})\frac{\partial}{\partial\theta}\delta u - (\frac{Y_{\theta z}}{2R^2})\frac{\partial^2}{\partial\theta^2}\delta u - (\frac{Y_{zx}}{2R})\frac{\partial^2}{\partial\theta\partial x}\delta u \\[2mm] +(\frac{Y_{\theta\theta}}{2R} - \frac{Y_{xx}}{2R})\frac{\partial}{\partial x}\delta v + (\frac{Y_{xz}}{2})\frac{\partial^2}{\partial x^2}\delta v - (\frac{Y_{\theta x}}{2R^2})\frac{\partial}{\partial\theta}\delta v \\[2mm] +(\frac{Y_{\theta z}}{2R})\frac{\partial^2}{\partial\theta\partial x}\delta v + (\frac{Y_{xz}}{2R^2})\delta v + (\frac{Y_{\theta z}}{2R})\frac{\partial}{\partial x}\delta w - (\frac{Y_{\theta x}}{2})\frac{\partial^2}{\partial x^2}\delta w \\[2mm] -(\frac{Y_{zx}}{2R^2})\frac{\partial}{\partial\theta}\delta w + (\frac{Y_{x\theta}}{2R^2})\frac{\partial^2}{\partial\theta^2}\delta w + (-\frac{Y_{\theta\theta}}{2R} + \frac{Y_{xx}}{2R})\frac{\partial^2}{\partial\theta\partial x}\delta w \\[2mm] +(\frac{Y_{x\theta}}{2})\frac{\partial}{\partial x}\delta\psi_x + (\frac{Y_{\theta\theta}}{2R} - \frac{Y_{xx}}{2R})\frac{\partial}{\partial\theta}\delta\psi_x - (\frac{T_{zx}}{2R})\frac{\partial^2}{\partial\theta\partial x}\delta\psi_x \\[2mm] -(\frac{Y_{z\theta}}{2R})\delta\psi_x - (\frac{Y_{x\theta}}{2R})\frac{\partial}{\partial\theta}\delta\psi_\theta + (\frac{Y_{\theta\theta}}{2R} - \frac{Y_{xx}}{2} + \frac{Y_{zz}}{2})\frac{\partial}{\partial x}\delta\psi_\theta \\[2mm] +(\frac{T_{z\theta}}{2R})\frac{\partial^2}{\partial\theta\partial x}\delta\psi_\theta - (\frac{T_{z\theta}}{2R^2})\frac{\partial^2}{\partial\theta^2}\delta\psi_x + (\frac{T_{xz}}{2})\frac{\partial^2}{\partial x^2}\delta\psi_\theta - (\frac{Y_{xz}}{2R})\delta\psi_\theta \end{array} \right\} Rdxd\theta \qquad (15)$$

where the classical and non-classical force and momentum are defined as follows:

$$(N_{xx},N_{\theta\theta},N_{x\theta}) = \int_{-\hat{z}_c}^{h-\hat{z}_c}(\sigma_{xx},\sigma_{\theta\theta},\sigma_{x\theta})dz,$$

$$(M_{xx},M_{\theta\theta},M_{x\theta}) = \int_{-\hat{z}_c}^{h-\hat{z}_c}(\sigma_{xx},\sigma_{\theta\theta},\sigma_{x\theta})zdz,$$

$$(Q_{xz},Q_{z\theta}) = \int_{-\hat{z}_c}^{h-\hat{z}_c}k_s(\sigma_{xz},\sigma_{z\theta})dz, \qquad (16)$$

$$(Y_{xx},Y_{\theta\theta},Y_{zz},Y_{x\theta},Y_{xz},Y_{z\theta}) = \int_{-\hat{z}_c}^{h-\hat{z}_c}(m_{xx},m_{\theta\theta},m_{zz},m_{x\theta},m_{xz},m_{z\theta})dz,$$

$$(T_{xx},T_{\theta\theta},T_{zz},T_{x\theta},T_{xz},T_{z\theta}) = \int_{-\hat{z}_c}^{h-\hat{z}_c}(m_{xx},m_{\theta\theta},m_{zz},m_{x\theta},m_{xz},m_{z\theta})zdz$$

Hamilton principle is used to find the equations of motions. Therefore, velocity vectors and position of a rotating cylindrical shell element are defined as follows [16]:

$$V = \frac{\partial u}{\partial t}i + (\frac{\partial v}{\partial t} + \Omega w)j + (\frac{\partial w}{\partial t} - \Omega v)k \qquad (17)$$

$\vec{i}, \vec{j}$ and $\vec{k}$ respectively are unit vectors in the $x$, $\theta$ and $z$ directions. Consequently, the kinetic energy of the rotating cylindrical shell can be written as:

$$\delta T = \iint_{Z} \iint_{A} \rho \left\{ \begin{array}{l} (\frac{\partial u}{\partial t} + z\,\frac{\partial \psi_x}{\partial t})(\frac{\partial}{\partial t}\delta u + z\,\frac{\partial}{\partial t}\delta \psi_x) + (\frac{\partial v}{\partial t} + z\,\frac{\partial \psi_\theta}{\partial t})(\frac{\partial}{\partial t}\delta v + z\,\frac{\partial}{\partial t}\delta \psi_\theta) \\[4pt] +(\frac{\partial w}{\partial t})\frac{\partial}{\partial t}\delta w + \Omega \left[ \begin{array}{l} w\,(\frac{\partial}{\partial t}\delta v + z\,\frac{\partial}{\partial t}\delta \psi_\theta) - (v + z\,\psi_\theta)(\frac{\partial}{\partial t}\delta w) + \\[4pt] \delta w\,(\frac{\partial v}{\partial t} + z\,\frac{\partial \psi_\theta}{\partial t}) - (\delta v + z\,\delta \psi_\theta)(\frac{\partial}{\partial t}w) \end{array} \right] + \\[4pt] \Omega^2 \left[ (v + z\,\psi_\theta)(\delta v + z\,\delta \psi_\theta) + w\,\delta w \right] \end{array} \right\} R\,dz\,dx\,d\theta \qquad (18)$$

Furthermore, initial hoop tension produced owing to centrifugal force of rotation is considered in potential energy. It is worth mentioning that the potential energy is obtained using nonlinear terms of thin Sanders theory in strain relations as recommended in Ref [16].

$$\delta U_h = \iint_{A} N_h \left\{ \left( \frac{\partial w}{R\,\partial \theta} - \frac{v}{R} \right) \left( \frac{\partial}{R\,\partial \theta}\delta w - \frac{\delta v}{R} \right) + \frac{1}{4} \left( \frac{\partial u}{R\,\partial \theta} - \frac{\partial v}{\partial x} \right) \left( \frac{\partial}{R\,\partial \theta}\delta u - \frac{\partial}{\partial x}\delta v \right) \right\} R\,d\theta\,dx \qquad (19)$$

In above equation $N_h = \int_{-\hat{z}_c}^{h-\hat{z}_c} \rho(z)R^2\Omega^2$ . Now by substituting Eqs. (15), (18) and (19) into (14) and integrating by parts, governing equations and boundary conditions using the FSDT shell model and the modified couple stress theory can be obtained. Appendix describes the governing equations and boundary conditions.

## 3   SOLUTION PROCEDURE

Bellman et al. introduced differential quadrature method (DQM) in the early 1970's [41, 42] as an reliable and effective method. The number of grid points controls the precision of the weighting coefficients leads to the accuracy of DQM. In the preliminary formulations of DQM, weighting coefficients were calculated by an algebraic equation system. This limits the number of grid points. Shu [43] devised an explicit formula for the weighting coefficients with infinite number of grid points leading to GDQM. Early applications of GDQ were applied mostly to regular domain problems. Shu and Richards [44] developed a domain decomposition technique to be used in the multi-domain problems. By this method, the main domain is divided into a number of sub-domains or elements, before discretizing each sub-domain for using GDQ. The *r-th* order derivative of function $f\left(x_i\right)$ can be expressed as follow:

$$\left. \frac{\partial^r f(x)}{\partial x^r} \right|_{x = x_p} = \sum_{j=1}^{n} C_{ij}^{(r)} f(x_i) \qquad (20)$$

where "$n$" is the number of grid points along "$x$" direction. Also, "$C_{ij}$" is obtained as follows:

$$C_{ij}^{(1)} = \frac{M(x_i)}{(x_i - x_j)M(x_j)} \qquad i,j = 1,2,...,n \quad \text{and} \quad i \neq j$$

$$C_{ij}^{(1)} = -\sum_{j=1,i\neq j}^{n} C_{ij}^{(1)} \qquad i = j \qquad\qquad (21)$$

where $M(x)$ is developed as:

$$M(x_i) = \prod_{j=1,j\neq i}^{n} (x_i - x_j) \qquad (22)$$

Superscript "$r$" is the order of the derivative. Also, $C^{(r)}$ is the weighing coefficient along $x$ direction, which is written as follows:

$$C_{ij}^{(r)} = r\left[C_{ij}^{(r-1)}C_{ij}^{(1)} - \frac{C_{ij}^{(r-1)}}{\left(x_i - x_j\right)}\right] \qquad i,j = 1,2,...,n, i \neq j \text{ and } 2 \leq r \leq n-1$$

$$C_{ii}^{(r)} = -\sum_{j=1,i\neq j}^{n} C_{ij}^{(r)} \qquad i,j = 1,2,...,n \text{ and } 1 \leq r \leq n-1$$

(23)

Owing to the geometrical periodicity of the cylindrical shell, the displacement vector for the free vibration analysis can be described as follow:

$$\begin{Bmatrix} u(x,\theta,t) \\ v(x,\theta,t) \\ w(x,\theta,t) \\ \psi_x(x,\theta,t) \\ \psi_\theta(x,\theta,t) \end{Bmatrix} = \sum_{n=1}^{\infty} \begin{Bmatrix} \overline{U}(x)\cos(n\theta)e^{i\omega t} \\ \overline{V}(x)\sin(n\theta)e^{i\omega t} \\ \overline{W}(x)\cos(n\theta)e^{i\omega t} \\ \overline{\Psi}_x(x)\cos(n\theta)e^{i\omega t} \\ \overline{\Psi}_\theta(x)\sin(n\theta)e^{i\omega t} \end{Bmatrix}$$

(24)

A proper method to discretize the domain is applying Chebyshev polynomials as it is explained in [45]. Now the following equation is obtained by substituting Eq. (24) into governing equations:

$$[M]\{\omega^2\} + [C]\{\omega\} + [K] = \{0\}$$

(25)

Stiffness matrix $[K]$, damping matrix $[C]$ and mass matrix $[M]$ are obtained by applying GDQ into the equations of motion and the boundary conditions. Eventually the natural frequency and its mode shape are obtained.

## 4 RESULTS

The numerical results of the vibration behavior of rotary FG cylindrical nanoshell are investigated based on the MCST with considering the initial hoop tension effects for the various boundary conditions. Sufficient number of grid points is necessary to achieve accurate results in GDQ method. As it is shown in Table 1., for the good results, fifteen grid points are appropriate. The Results are shown and analyzed in two sections. The first one verifies proposed model with existing literatures. Second section shows the effect of length to radius ratio, angular velocity, material length scale parameter, FG power index, and boundary conditions on critical speed and natural frequency of the rotating cylindrical FG nanoshell.

**Table1**
The effect of the number of grid points on evaluating convergence of the non-dimensional natural frequency of the FG cylindrical nanoshell with respect to the different dimensionless angular velocity, boundary conditions (B.Cs) and *L/R*=0.375, *h/R*=0.2, *l*=*R*/3.

| B.Cs | Angular velocity | *N*=5 | *N*=7 | *N*=9 | *N*=11 | *N*=13 | *N*=15 | *N*=17 | *N*=19 |
|---|---|---|---|---|---|---|---|---|---|
| Simply-Simply | $\Phi$ =0.1 | 0.9094 | 0.9086 | 0.9092 | 0.9191 | 0.9191 | 0.9191 | 0.9191 | 0.9191 |
| | $\Phi$ =0.3 | 0.8655 | 0.8645 | 0.8651 | 0.8651 | 0.8651 | 0.8651 | 0.8651 | 0.8651 |
| Simply-Clamp | $\Phi$ =0.1 | 1.0037 | 1.0045 | 1.0040 | 1.0037 | 1.0036 | 1.0035 | 1.0035 | 1.0035 |
| | $\Phi$ =0.3 | 0.9605 | 0.9612 | 0.9607 | 0.9603 | 0.9602 | 0.9602 | 0.9602 | 0.9602 |
| Clamp-Clamp | $\Phi$ =0.1 | 1.1753 | 1.1719 | 1.1725 | 1.1719 | 1.1717 | 1.1717 | 1.1717 | 1.1717 |
| | $\Phi$ =0.3 | 1.1229 | 1.1196 | 1.1202 | 1.1196 | 1.1195 | 1.1194 | 1.1194 | 1.1194 |
| Clamp-Free | $\Phi$ =0.1 | 0.5066 | 0.5057 | 0.5063 | 0.5063 | 0.5063 | 0.5063 | 0.5063 | 0.5063 |
| | $\Phi$ =0.3 | 0.4673 | 0.4665 | 0.4670 | 0.4670 | 0.4670 | 0.4670 | 0.4670 | 0.4670 |

*4.1 Results verification with MD simulation*

There is no research on cylindrical FG nanoshell in the field of MD simulation, when the research, which have been done by now, are considered. Therefore, the value of *N* is set to zero so that the findings of proposed MD simulation

can be compared with other literatures. In addition, Material properties of single-walled carbon nanotubes are presented in Table1. Now achieved results of MD simulation are compared with those of GDQ and exact analytical method. Moreover in Tables 3., and 4, it can be seen from the results that by setting $L = h$, the achieved results of classical cylindrical nanoshell theory are very close to MD simulation results. Some researchers [1, 46] show, as $l=R/3$, the results of the current research based on FSDT are very similar to those of MD simulation. In addition, dimensionless frequency in this article, is approximated by Eq. $\Omega = \omega R \sqrt{\dfrac{\rho}{E}}$ .

**Table2**
Material properties of single-walled carbon nanotubes.

| $E$ | $v$ | $H$ | $\rho$ |
|---|---|---|---|
| *1.1 Tpa* | *0.3* | *0.34 nm* | $2300 kg \ / \ m^3$ |

**Table3**
Comparison of dimensionless first natural frequencies of non rotating simply supported isotropic homogeneous nano shells, with different thicknesses.

| h/R | N | MD simulation [47] | Present GDQM (*l*=0) | Present Analytical (*l*=0) | Present GDQM (*l*=h) | Present Analytical (*l*=h) |
|---|---|---|---|---|---|---|
| 0.02 | 1 | 0.1968 | 0.1953621557 | 0.1953621467 | 0.19543206 | 0.1954320689 |
| 0.05 | 1 | 0.2004 | 0.1954230464 | 0.1954230557 | 0.1958578181 | 0.1958578259 |

**Table4**
Comparison of dimensionless first three natural frequencies ofsimply supported isotropic homogeneous nano shells, with different thicknesses.

| h/R | N | Ref [48] (*l*=0) | Present study (GDQM) (*l*=0) | Ref [48] (*l*=h) | Present study (GDQM) (*l*=h) |
|---|---|---|---|---|---|
| | 1 | 0.1954 | 0.19536215 | 0.1955 | 0.19543206 |
| 0.02 | 2 | 0.2532 | 0.25271274 | 0.2575 | 0.25731258 |
| | 3 | 0.2772 | 0.27580092 | 0.3067 | 0.30621690 |
| | 1 | 0.1959 | 0.19542305 | 0.1963 | 0.19585782 |
| 0.05 | 2 | 0.2623 | 0.25884786 | 0.2869 | 0.28543902 |
| | 3 | 0.3220 | 0.31407326 | 0.4586 | 0.45457555 |

*4.2 Verification of achieved results by using the results of an analytical method*

Fig.3 demonstrates the GDQ results in comparison with analytical results for different materials including ceramic and metal. It can be seen from figure3 that the GDQ results are in accord with analytical results, so the GDQ method with *N*=15 can be used instead of analytical solution. Also, In Fig. 3 it can be seen that, by increasing the length, natural frequency tends to decrease and by increasing the FG power index, the natural frequency increase. Comparison of the natural frequencies obtained in three illustrations shows that increase in shell length leads to decrease in stiffness and therefore decrease in natural frequency.
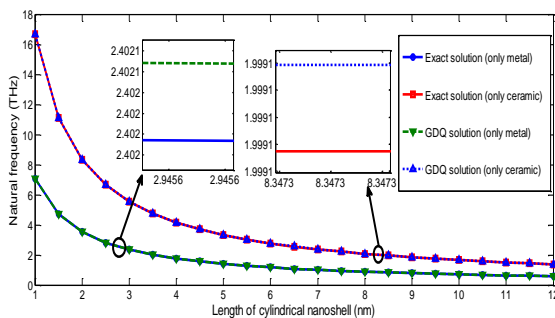


**Fig.3**
Comparison of fundamental natural frequency of simply supported FG nanoshells, with different Length.

*4.3 Parametric results*

The material for this paper is functionally graded and it is assumed that the Inner surface is ceramic and the outer one is metal. Volume fraction index (*n*) determines the variation profile of the material properties across the thickness of the rotary FG cylindrical nanoshell. The material properties are given in Table 5.

Table 6., gives a presentation of circumferential wave numbers, angular velocity, and FG power index effect on natural frequency under the various boundary conditions. As it can be seen from Table 5., an increase in FG power index leads to an increase in the frequency of all modes. This trend is observed under all types of boundary conditions. In addition, the increase in the modes of the frequency results in considerable increase in natural frequency. Clamp-Free boundary condition has the lowest frequency because of its particular condition, and Clamp-Clamp boundary condition has the highest frequency. Also it can be seen from the Fig.5 that in fundamental frequency, the increase in angular speed leads to the decrease in the frequency. A surprising result is that unlike C-C , C-S, and S-S boundary, under C-F boundary condition, an increase in rotational speed results in a decrease in second frequency mode as the same as first frequency mode. In third frequency, an increase in rotational speed leads to an increase in frequency. This happens under all types of boundary condition. Table 7., demonstrates the effect of angular velocities, length to radius ratio and material length scale parameter on natural frequency for various boundary conditions. It is observed that by increasing the length-to-radius ratio, the natural frequency tends to decrease. From the results of Table 6., it is observed that by increasing the material length scale parameter, the natural frequency increase. Also, by increasing the length to radius ratio the natural frequency increases. This is because increasing the length to radius ratio is eventuated to decrease in stiffness and natural frequency of the rotating FG cylindrical nanoshell.

**Table 5**
Material properties of FGM constituents.

| Material properties | Unit | Aluninum | Silicon |
|---|---|---|---|
| $E$ | *GPa* | 70 | 210 |
| $\rho$ | *$Kg/m^3$* | 2700 | 2370 |
| $v$ | | 0.3 | 0.24 |

**Table 6**
Variation of the nondimensional fundamental and the second frequency, with different volume fraction of a rotating FG cylindrical nanoshell for different dimensionless angular velocities and boundary conditions with *L/R*=0.375, *h/R*=0.2 and *l =R/3*.

| | Fundamental frequency | | | Second frequency | | | Third frequency | | |
|---|---|---|---|---|---|---|---|---|---|
| | $\Phi =0$ | 0.3 | 0.5 | $\Phi =0$ | 0.3 | 0.5 | $\Phi =0$ | 0.3 | 0.5 |
| Simply_Simply *N* | | | | | | | | | |
| Metal | 0.49612 | 0.46815 | 0.40409 | 0.65646 | 0.65925 | 0.66378 | 1.37499 | 1.58684 | 1.84162 |
| 1 | 0.91418 | 0.86508 | 0.75268 | 1.22782 | 1.24636 | 1.25382 | 2.58149 | 2.98734 | 3.45998 |
| 5 | 1.09521 | 1.03644 | 0.90223 | 1.47250 | 1.48410 | 1.49156 | 3.09215 | 3.56136 | 4.09660 |
| Ceramic | 1.17296 | 1.10958 | 0.96504 | 1.57204 | 1.57615 | 1.59380 | 3.30483 | 3.79383 | 4.34399 |
| Simply_Clamp *N* | | | | | | | | | |
| Metal | 0.54366 | 0.51598 | 0.45035 | 0.72799 | 0.73791 | 0.74539 | 1.41902 | 1.64377 | 1.90617 |
| 1 | 1.00871 | 0.96020 | 0.84475 | 1.36381 | 1.38716 | 1.40807 | 2.66417 | 3.09229 | 3.57121 |
| 5 | 1.21229 | 1.15414 | 1.01600 | 1.63457 | 1.62995 | 1.61626 | 3.18786 | 3.68038 | 4.21799 |
| Ceramic | 1.30004 | 1.23453 | 1.07702 | 1.74850 | 1.76872 | 1.78422 | 3.40483 | 3.91685 | 4.46711 |
| Clamp_Clamp *N* | | | | | | | | | |
| Metal | 0.62887 | 0.59580 | 0.51361 | 0.81811 | 0.83171 | 0.84006 | 1.47583 | 1.72165 | 1.99534 |
| 1 | 1.17802 | 1.12003 | 0.97278 | 1.53528 | 1.56508 | 1.58558 | 2.77113 | 3.2352 | 3.71782 |
| 5 | 1.41879 | 1.34959 | 1.17355 | 1.83692 | 1.86732 | 1.88201 | 3.30953 | 3.84502 | 4.37674 |
| Ceramic | 1.52199 | 1.44742 | 1.25791 | 1.96234 | 1.99077 | 1.99904 | 3.53061 | 4.07573 | 4.61621 |
| Clamp_Free *N* | | | | | | | | | |
| Metal | 0.27576 | 0.25089 | 0.19999 | 0.58567 | 0.58337 | 0.57792 | 1.31919 | 1.52606 | 1.78518 |
| 1 | 0.51199 | 0.45903 | 0.34745 | 1.08987 | 1.08667 | 1.07705 | 2.47501 | 2.86629 | 3.32655 |
| 5 | 0.61782 | 0.56359 | 0.45049 | 1.30181 | 1.29867 | 1.28364 | 2.95257 | 3.40214 | 3.90194 |
| Ceramic | 0.66544 | 0.60698 | 0.48980 | 1.39338 | 1.39199 | 1.37492 | 3.14979 | 3.61958 | 4.11825 |

**Table7**
Variation of the fundamental frequency (THz), with *h/R* and *L/R* ratioes of a rotating FG cylindrical nanoshell for different angular velocities, material length scale parameter and boundary conditions and *N*=1.

| B.Cs | $\phi$ =0THz | | | | $\phi$ =5THz | | | |
|---|---|---|---|---|---|---|---|---|
| | *L/R*=3 | | *L/R*=5 | | *L/R*=3 | | *L/R*=5 | |
| Simply_Simply | *l=0* | *l=R/3.* | *l=0* | *l=R/3.* | *l=0* | *l=R/3.* | *l=0* | *l=R/3.* |
| *h/R* | | | | | | | | |
| 0.1 | 10.9724 | 12.4292 | 9.11337 | 9.85833 | 9.20997 | 10.9505 | 6.24595 | 7.32752 |
| 0.2 | 11.0352 | 12.4662 | 9.14543 | 9.88168 | 9.30630 | 11.0096 | 6.30522 | 7.36985 |
| 0.3 | 11.1286 | 12.5266 | 9.19698 | 9.92333 | 9.43902 | 11.0656 | 6.39281 | 7.43682 |
| Simply_Clamp | | | | | | | | |
| *h/R* | | | | | | | | |
| 0.1 | 11.4292 | 13.8666 | 10.4825 | 11.8821 | 9.80885 | 12.6560 | 8.11551 | 9.89205 |
| 0.2 | 11.6138 | 13.9032 | 10.5814 | 11.9128 | 10.0534 | 12.7121 | 8.25378 | 9.93671 |
| 0.3 | 11.8368 | 13.9614 | 10.7036 | 11.9640 | 10.3409 | 12.7926 | 8.42132 | 10.0061 |
| Clamp_Clamp | | | | | | | | |
| *h/R* | | | | | | | | |
| 0.1 | 12.3910 | 16.1866 | 12.0225 | 14.1734 | 10.9023 | 15.1569 | 9.99647 | 12.5290 |
| 0.2 | 12.7370 | 16.2379 | 12.2024 | 14.2162 | 11.3254 | 15.2238 | 10.2234 | 12.5826 |
| 0.3 | 13.1403 | 16.3092 | 12.4128 | 14.2821 | 11.8078 | 15.3127 | 10.4806 | 12.6624 |
| Clamp_Free | | | | | | | | |
| *h/R* | | | | | | | | |
| 0.1 | 5.15514 | 6.91505 | 4.25612 | 5.78072 | 3.18154 | 0.87196 | 3.70128 | 4.03570 |
| 0.2 | 5.41698 | 7.00267 | 4.53263 | 5.91723 | 1.07119 | 0.70048 | 2.47304 | 3.82191 |
| 0.3 | 5.66164 | 7.06662 | 4.78742 | 5.99276 | 2.57131 | 1.18536 | 0.93126 | 3.69941 |

   Figs. 4-7 show the effect of the length to radius ratio on critical speed of cylindrical FG nanoshell with different boundary conditions. It can be seen from Figs. 4-7 that the increase in *L/R* leads to the increase in critical speed and consequently the increase in stability of the system. Moreover, the C-F boundary condition results in instability in lower critical speed, in spite of C-F boundary condition, C-C boundary condition leads to instability in higher critical speed. Figs. 8-11 demonstrate the effect of material length scale parameter on critical speed under different boundary conditions. It can be seen from these figure that an increase in material length scale parameter leads to an increase in critical speed value so that instability occurs in higher value of critical speed. Therefore, the higher the length scale value, the more stable the system. Also, the results of C-F boundary condition in instability in lower critical speed, in spite of C-F boundary condition, C-C boundary condition leads to instability in higher critical speed.
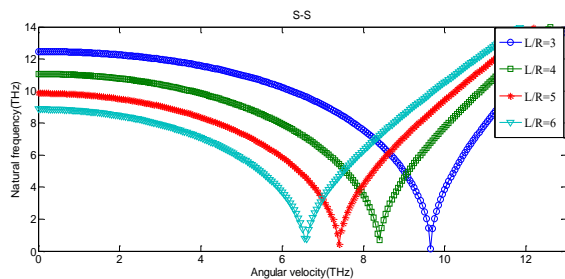


**Fig.4**
Variation of fundamental frequency (THz) with angular velocity of a rotating Simply- Simply cylindrical FG nanoshell with different length to radius ratios with *h/R*=0.2 and *l=R/3* and *n=N*=1 and *L*=1*nm*.
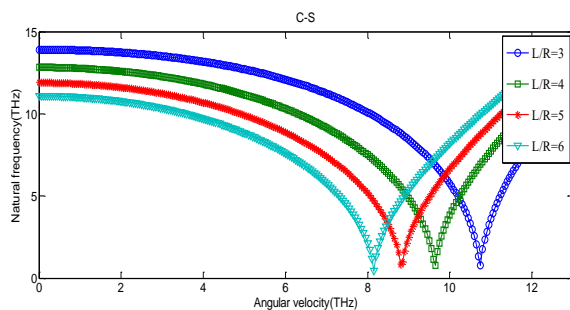


**Fig.5**
Variation of fundamental frequency (THz) with angular velocity of a rotating clamp-Simply cylindrical FG nanoshell with different length to radius ratios for with *h/R*=0.2 and *l=R/3* and *n=N*=1 and *L*=1*nm*.
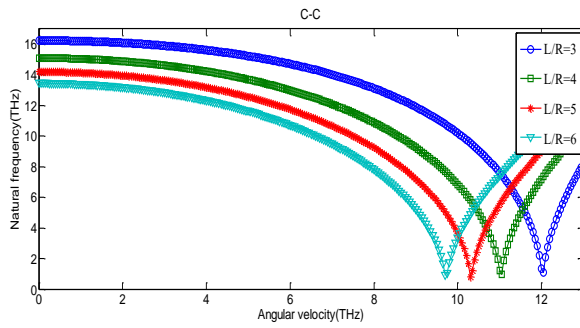
**Fig.6**
Variation of fundamental frequency (THz) with angular velocity of a rotating clamp-clamp cylindrical FG nanoshell with different length to radius ratios for with *h/R*=0.2 and *l*=*R*/3 and *n*=*N*=1 and *L*=1*nm*.
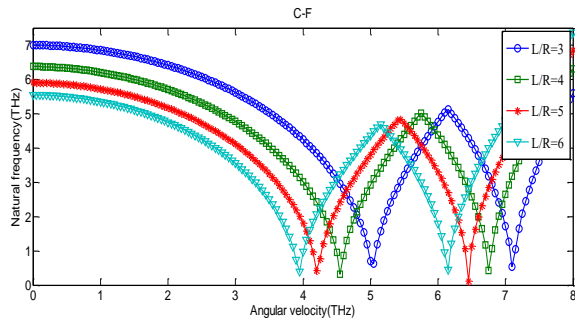


**Fig.7**
Variation of fundamental frequency (THz) with angular velocity of a rotating clamp-free cylindrical FG nanoshell with different length to radius ratios for with *h/R*=0.2 and *l*=*R*/3 and *n*=*N*=1 and *L*=1*nm*.
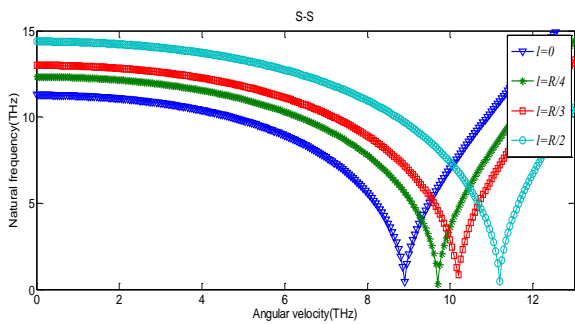


**Fig.8**
Variation of fundamental frequency (THz) with angular velocity of a rotating Simply- Simply cylindrical FG nanoshell with different length scale parameter with *h/R*=0.2 and *l*=*R**.375 and *n*=*N*=1 and *L*=1*nm*.
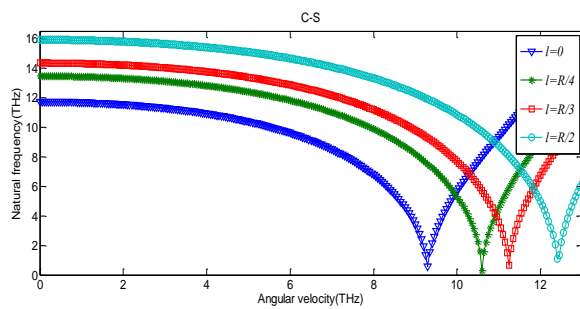


**Fig.9**
Variation of fundamental frequency (THz) with angular velocity of a rotating Simply- Clamp cylindrical FG nanoshell with different length scale parameter with *h/R*=0.2 and *l*=*R**.375 and *n*=*N*=1 and *L*=1*nm*.
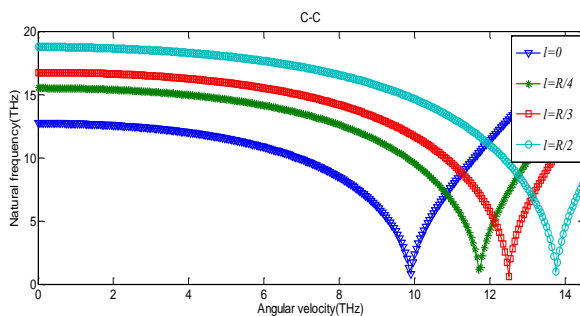


**Fig.10**
Variation of fundamental frequency (THz) with angular velocity of a rotating Clamp- Clamp cylindrical FG nanoshell with different length scale parameter with *h/R*=0.2 and *l*=*R**.375 and *n*=*N*=1 and *L*=1*nm*.
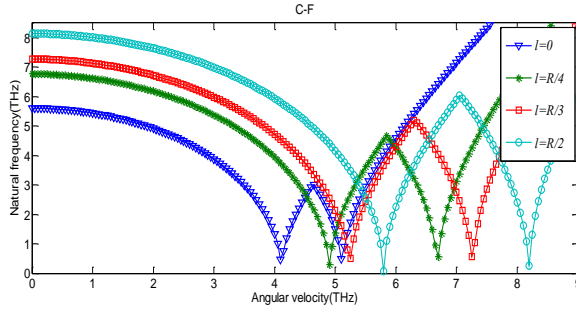
**Fig.11**
Variation of fundamental frequency (THz) with angular velocity of a rotating Clamp- Free cylindrical FG nanoshell with different length scale parameter with *h/R*=0.2 and *l=R*\*.375 and *n=N*=1 and *L*=1*nm*.

## 5   CONCLUSIONS

This paper presents the free vibration analysis of a rotary functionally graded cylindrical nanoshell modeled by considering initial hoop tension effect. Modified couple stress theory introduces the size-dependent effect. The equations of motion and non-classic boundary conditions are derived using Hamilton's principle. The natural frequency of the rotating FG cylindrical nanoshell are investigated with respect to the material length scale parameter, angular velocity, length to radius ratio and FG power index for different boundary conditions of the cylindrical FG nanoshell. The followings important results can be obtained from this study:

1. By increasing the length to radius ratio, FG power index and material length scale parameter the natural frequency tend to increase.
2. A surprising result is that unlike C-C , C-S, and S-S boundary, under C-F boundary condition, an increase in rotational speed results in a decrease in second frequency mode as the same as first  frequency mode.
3. Clamp-Free boundary condition has the lowest natural frequency because of its particular condition, and Clamp-Clamp boundary condition has the highest natural frequency.
4. The results show that, increase in the length to radius ratio and material length scale parameter lead to increase in the critical speed of the rotation FG cylindrical nanoshell.

## APPENDIX A

The governing equations of the rotation FG cylindrical nanoshell are as bellow:

$$
\begin{aligned}
\delta u : & \frac{\partial}{\partial x}\left\{A_{11}\frac{\partial u}{\partial x}+B_{11}\frac{\partial \psi_x}{\partial x}+A_{12}\left(\frac{\partial v}{R\partial \theta}+\frac{w}{R}\right)+B_{12}\frac{\partial \psi_\theta}{R\partial \theta}\right\}+\frac{1}{R}\frac{\partial}{\partial \theta}\left\{A_{55}(\frac{1}{R}\frac{\partial u}{\partial \theta}+\frac{\partial v}{\partial x})+B_{55}(\frac{1}{R}\frac{\partial \psi_x}{\partial \theta}+\frac{\partial \psi_\theta}{\partial x})\right\}- \\
& \frac{1}{2R^2}\frac{\partial}{\partial \theta}\left\{-A_{55}l^2\left[\frac{1}{R}(\frac{1}{R}\frac{\partial u}{\partial \theta}-\frac{\partial v}{\partial x})+\frac{1}{R}\frac{\partial^2 w}{\partial x\partial \theta}-\frac{1}{R}\frac{\partial \psi_x}{\partial \theta}\right]-B_{55}l^2(-\frac{\partial \psi_\theta}{\partial x})\right\}+ \\
& \frac{1}{2R^2}\frac{\partial}{\partial \theta}\left\{-A_{55}l^2\left[-\frac{1}{R^2}\frac{\partial u}{\partial \theta}+\frac{1}{R}\frac{\partial \psi_x}{\partial \theta}-\frac{\partial \psi_\theta}{\partial x}\right]\right\}+ \\
& \frac{1}{2R}\frac{\partial^2}{\partial \theta\partial x}\left\{-\frac{A_{55}l^2}{2}\left[-\frac{\partial^2 v}{\partial x^2}-\frac{v}{R^2}+\frac{1}{R}\frac{\partial^2 u}{\partial x\partial \theta}+\frac{\psi_\theta}{R}+\frac{1}{R^2}\frac{\partial w}{\partial \theta}\right]-\frac{B_{55}l^2}{2}(\frac{1}{R}\frac{\partial^2 \psi_x}{\partial x\partial \theta}-\frac{\partial^2 \psi_\theta}{\partial x^2}),\right\}+ \\
& \frac{1}{2R^2}\frac{\partial^2}{\partial \theta^2}\left\{-\frac{A_{55}l^2}{2}\left[\frac{1}{R^2}\frac{\partial^2 u}{\partial \theta^2}-\frac{1}{R}\frac{\partial^2 v}{\partial x\partial \theta}+\frac{\psi_x}{R}-\frac{1}{R}\frac{\partial w}{\partial x}\right]-\frac{B_{55}l^2}{2}(\frac{1}{R^2}\frac{\partial^2 \psi_x}{\partial \theta^2}-\frac{1}{R}\frac{\partial^2 \psi_y}{\partial x\partial \theta})\right\} \\
& -N_h(\frac{1}{R}\frac{\partial^2 v}{\partial x\partial \theta}-\frac{1}{R^2}\frac{\partial^2 u}{\partial \theta^2})=I_0\frac{\partial^2 u}{\partial t^2}+I_1\frac{\partial^2 \psi_x}{\partial t^2}
\end{aligned}
\tag{A.1}
$$

$$\delta v : \frac{\partial}{\partial x}\left\{A_{55}(\frac{1}{R}\frac{\partial u}{\partial \theta}+\frac{\partial v}{\partial x})+B_{55}(\frac{1}{R}\frac{\partial \psi_x}{\partial \theta}+\frac{\partial \psi_\theta}{\partial x})\right\}+$$

$$\frac{1}{R}\frac{\partial}{\partial \theta}\left\{A_{11}(\frac{w}{R}+\frac{1}{R}\frac{\partial v}{\partial \theta})+B_{11}\frac{1}{R}\frac{\partial \psi_\theta}{\partial \theta}+A_{12}\frac{\partial u}{\partial x}+B_{12}\frac{\partial \psi_x}{\partial x}\right\}$$

$$+\frac{1}{R}\left\{k_s A_{55}(\psi_\theta+\frac{1}{R}\frac{\partial w}{\partial \theta}-\frac{v}{R})\right\}-\frac{1}{2R}\frac{\partial}{\partial x}\left\{-A_{55}l^2(\frac{\partial \psi_\theta}{\partial x}+\frac{1}{R}\frac{\partial v}{\partial x}-\frac{1}{R}\frac{\partial^2 w}{\partial x \partial \theta})\right\}$$

$$+\frac{1}{2R}\frac{\partial}{\partial x}\left\{-A_{55}l^2\left[\frac{1}{R}(\frac{1}{R}\frac{\partial u}{\partial \theta}-\frac{\partial v}{\partial x})+\frac{1}{R}\frac{\partial^2 w}{\partial x \partial \theta}-\frac{1}{R}\frac{\partial \psi_x}{\partial \theta}\right]-B_{55}l^2(-\frac{\partial \psi_\theta}{\partial x})\right\}$$

$$-\frac{1}{R^2}\frac{\partial}{\partial \theta}\left\{-\frac{A_{55}l^2}{4}(\frac{1}{R^2}\frac{\partial v}{\partial \theta}+\frac{\partial^2 w}{\partial x^2}-\frac{1}{R^2}\frac{\partial^2 w}{\partial \theta^2}+\frac{1}{R}\frac{\partial \psi_\theta}{\partial \theta}-\frac{\partial \psi_x}{\partial x})\right\}$$

(A.2)

$$-\frac{\partial^2}{\partial x^2}\left\{-\frac{A_{55}l^2}{4}\left[-\frac{\partial^2 v}{\partial x^2}-\frac{v}{R^2}+\frac{1}{R}\frac{\partial^2 u}{\partial x \partial \theta}+\frac{\psi_\theta}{R}+\frac{1}{R^2}\frac{\partial w}{\partial \theta}\right]-\frac{B_{55}l^2}{4}(\frac{1}{R}\frac{\partial^2 \psi_x}{\partial x \partial \theta}-\frac{\partial^2 \psi_\theta}{\partial x^2})\right\}$$

$$-\frac{1}{R^2}\left\{-\frac{A_{55}l^2}{4}\left[-\frac{\partial^2 v}{\partial x^2}-\frac{v}{R^2}+\frac{1}{R}\frac{\partial^2 u}{\partial x \partial \theta}+\frac{\psi_\theta}{R}+\frac{1}{R^2}\frac{\partial w}{\partial \theta}\right]-\frac{B_{55}l^2}{4}(\frac{1}{R}\frac{\partial^2 \psi_x}{\partial x \partial \theta}-\frac{\partial^2 \psi_\theta}{\partial x^2})\right\}$$

$$-\frac{1}{R}\frac{\partial^2}{\partial \theta \partial x}\left\{-\frac{A_{55}l^2}{4}\left[\frac{1}{R^2}\frac{\partial^2 u}{\partial \theta^2}-\frac{1}{R}\frac{\partial^2 v}{\partial x \partial \theta}+\frac{\psi_x}{R}-\frac{1}{R}\frac{\partial w}{\partial x}\right]-\frac{B_{55}l^2}{4}(\frac{1}{R^2}\frac{\partial^2 \psi_x}{\partial \theta^2}-\frac{1}{R}\frac{\partial^2 \psi_y}{\partial x \partial \theta})\right\}$$

$$-N_h(\frac{1}{R}\frac{\partial^2 u}{\partial x \partial \theta}-\frac{\partial^2 v}{\partial x^2}+\frac{v}{R^2}-\frac{1}{R^2}\frac{\partial w}{\partial \theta})=I_0\left[\frac{\partial^2 v}{\partial t^2}+2(\frac{\partial w}{\partial t})\Omega-v\Omega^2\right]+I_1\left\{\frac{\partial^2 \psi_\theta}{\partial t^2}-\psi_\theta\Omega^2\right\}$$

$$\delta w : \frac{\partial}{\partial x}\left\{k_s A_{55}(\psi_x+\frac{\partial w}{\partial x})\right\}+\frac{1}{R}\frac{\partial}{\partial \theta}\left\{k_s A_{55}(\psi_\theta+\frac{1}{R}\frac{\partial w}{\partial \theta}-\frac{v}{R})\right\}-$$

$$\frac{1}{R}\left\{A_{11}(\frac{w}{R}+\frac{1}{R}\frac{\partial v}{\partial \theta})+B_{11}\frac{1}{R}\frac{\partial \psi_\theta}{\partial \theta}+A_{12}\frac{\partial u}{\partial x}+B_{12}\frac{\partial \psi_x}{\partial x}\right\}-$$

$$\frac{1}{2R^2}\frac{\partial^2}{\partial \theta^2}\left\{-\frac{A_{55}l^2}{2}(\frac{1}{R^2}\frac{\partial v}{\partial \theta}+\frac{\partial^2 w}{\partial x^2}-\frac{1}{R^2}\frac{\partial^2 w}{\partial \theta^2}+\frac{1}{R}\frac{\partial \psi_\theta}{\partial \theta}-\frac{\partial \psi_x}{\partial x})\right\}-$$

$$\frac{1}{2R^2}\frac{\partial}{\partial \theta}\left\{-\frac{A_{55}l^2}{2}\left[-\frac{\partial^2 v}{\partial x^2}-\frac{v}{R^2}+\frac{1}{R}\frac{\partial^2 u}{\partial x \partial \theta}+\frac{\psi_\theta}{R}+\frac{1}{R^2}\frac{\partial w}{\partial \theta}\right]-\frac{B_{55}l^2}{2}(\frac{1}{R}\frac{\partial^2 \psi_x}{\partial x \partial \theta}-\frac{\partial^2 \psi_\theta}{\partial x^2})\right\}+$$

$$\frac{1}{2R}\frac{\partial}{\partial x}\left\{-\frac{A_{55}l^2}{2}\left[\frac{1}{R^2}\frac{\partial^2 u}{\partial \theta^2}-\frac{1}{R}\frac{\partial^2 v}{\partial x \partial \theta}+\frac{\psi_x}{R}-\frac{1}{R}\frac{\partial w}{\partial x}\right]-\frac{B_{55}l^2}{2}(\frac{1}{R^2}\frac{\partial^2 \psi_x}{\partial \theta^2}-\frac{1}{R}\frac{\partial^2 \psi_y}{\partial x \partial \theta})\right\}+$$

(A.3)

$$\frac{\partial^2}{2\partial x^2}\left\{-\frac{A_{55}l^2}{2}(\frac{1}{R^2}\frac{\partial v}{\partial \theta}+\frac{\partial^2 w}{\partial x^2}-\frac{1}{R^2}\frac{\partial^2 w}{\partial \theta^2}+\frac{1}{R}\frac{\partial \psi_\theta}{\partial \theta}-\frac{\partial \psi_x}{\partial x})\right\}$$

$$-\frac{1}{2R}\frac{\partial^2}{\partial \theta \partial x}\left\{-A_{55}l^2(\frac{\partial \psi_\theta}{\partial x}+\frac{1}{R}\frac{\partial v}{\partial x}-\frac{1}{R}\frac{\partial^2 w}{\partial x \partial \theta})\right\}+$$

$$\frac{1}{2R}\frac{\partial^2}{\partial \theta \partial x}\left\{-A_{55}l^2\left[\frac{1}{R}(\frac{1}{R}\frac{\partial u}{\partial \theta}-\frac{\partial v}{\partial x})+\frac{1}{R}\frac{\partial^2 w}{\partial x \partial \theta}-\frac{1}{R}\frac{\partial \psi_x}{\partial \theta}\right]-B_{55}l^2(-\frac{\partial \psi_\theta}{\partial x})\right\}$$

$$-N_h(\frac{1}{R^2}\frac{\partial v}{\partial \theta}-\frac{1}{R^2}\frac{\partial^2 w}{\partial \theta^2})=I_0(\frac{\partial^2 w}{\partial t^2}-2\Omega\frac{\partial v}{\partial t}-\Omega^2 w)-2I_1\left\{\Omega\frac{\partial \psi_\theta}{\partial t}\right\}$$

$$\delta\psi_x : \frac{\partial}{\partial x}\left\{B_{11}\frac{\partial u}{\partial x}+D_{11}\frac{\partial\psi_x}{\partial x}+B_{12}\left(\frac{\partial v}{R\,\partial\theta}+\frac{w}{R}\right)+D_{12}\frac{\partial\psi_\theta}{R\,\partial\theta}\right\}+$$

$$\frac{1}{R}\frac{\partial}{\partial\theta}\left\{B_{55}(\frac{1}{R}\frac{\partial u}{\partial\theta}+\frac{\partial v}{\partial x})+D_{55}(\frac{1}{R}\frac{\partial\psi_x}{\partial\theta}+\frac{\partial\psi_\theta}{\partial x})\right\}$$

$$-\left\{k_s A_{55}(\psi_x+\frac{\partial w}{\partial x})\right\}+\frac{1}{2}\frac{\partial}{\partial x}\left\{-\frac{A_{55}L^2}{2}(\frac{1}{R^2}\frac{\partial v}{\partial\theta}+\frac{\partial^2 w}{\partial x^2}-\frac{1}{R^2}\frac{\partial^2 w}{\partial\theta^2}+\frac{1}{R}\frac{\partial\psi_\theta}{\partial\theta}-\frac{\partial\psi_x}{\partial x})\right\}$$

$$-\frac{1}{2R}\frac{\partial}{\partial\theta}\left\{-A_{55}l^2\left[-\frac{1}{R^2}\frac{\partial u}{\partial\theta}+\frac{1}{R}\frac{\partial\psi_x}{\partial\theta}-\frac{\partial\psi_\theta}{\partial x}\right]\right\}+$$

$$\frac{1}{2R}\frac{\partial}{\partial\theta}\left\{-A_{55}l^2\left[\frac{1}{R}(\frac{1}{R}\frac{\partial u}{\partial\theta}-\frac{\partial v}{\partial x})+\frac{1}{R}\frac{\partial^2 w}{\partial x\,\partial\theta}-\frac{1}{R}\frac{\partial\psi_x}{\partial\theta}\right]-B_{55}l^2(-\frac{\partial\psi_\theta}{\partial x})\right\}$$

$$+\frac{1}{2R}\left\{\frac{A_{55}l^2}{2}\left[\frac{1}{R^2}\frac{\partial^2 u}{\partial\theta^2}-\frac{1}{R}\frac{\partial^2 v}{\partial x\,\partial\theta}+\frac{\psi_x}{R}-\frac{1}{R}\frac{\partial w}{\partial x}\right]-\frac{B_{55}l^2}{2}(\frac{1}{R^2}\frac{\partial^2\psi_x}{\partial\theta^2}-\frac{1}{R}\frac{\partial^2\psi_\theta}{\partial x\,\partial\theta})\right\} \tag{A.4}$$

$$+\frac{1}{2R}\frac{\partial^2}{\partial\theta\,\partial x}\left\{-\frac{B_{55}l^2}{2}\left[-\frac{\partial^2 v}{\partial x^2}-\frac{v}{R^2}+\frac{1}{R}\frac{\partial^2 u}{\partial x\,\partial\theta}+\frac{\psi_\theta}{R}+\frac{1}{R^2}\frac{\partial w}{\partial\theta}\right]-\frac{D_{55}l^2}{2}(\frac{1}{R}\frac{\partial^2\psi_x}{\partial x\,\partial\theta}-\frac{\partial^2\psi_\theta}{\partial x^2})\right\}$$

$$+\frac{1}{2R^2}\frac{\partial^2}{\partial\theta^2}\left\{-\frac{B_{55}l^2}{2}\left[\frac{1}{R^2}\frac{\partial^2 u}{\partial\theta^2}-\frac{1}{R}\frac{\partial^2 v}{\partial x\,\partial\theta}+\frac{\psi_x}{R}-\frac{1}{R}\frac{\partial w}{\partial x}\right]-\frac{D_{55}l^2}{2}(\frac{1}{R^2}\frac{\partial^2\psi_x}{\partial\theta^2}-\frac{1}{R}\frac{\partial^2\psi_\theta}{\partial x\,\partial\theta})\right\}=I_1\frac{\partial^2 u}{\partial t^2}+I_2\frac{\partial^2\psi_x}{\partial t^2}$$

$$\delta\psi_\theta : \frac{1}{R}\frac{\partial}{\partial\theta}\left\{B_{11}(\frac{w}{R}+\frac{1}{R}\frac{\partial v}{\partial\theta})+D_{11}\frac{1}{R}\frac{\partial\psi_\theta}{\partial\theta}+B_{12}\frac{\partial u}{\partial x}+D_{12}\frac{\partial\psi_x}{\partial x}\right\}+$$

$$\frac{\partial}{\partial x}\left\{B_{55}(\frac{1}{R}\frac{\partial u}{\partial\theta}+\frac{\partial v}{\partial x})+D_{55}(\frac{1}{R}\frac{\partial\psi_x}{\partial\theta}+\frac{\partial\psi_\theta}{\partial x})\right\}-k_s A_{55}(\psi_\theta+\frac{1}{R}\frac{\partial w}{\partial\theta}-\frac{v}{R})+$$

$$\frac{1}{2}\frac{\partial}{\partial x}\left\{-A_{55}l^2\left[-\frac{1}{R^2}\frac{\partial u}{\partial\theta}+\frac{1}{R}\frac{\partial\psi_x}{\partial\theta}-\frac{\partial\psi_\theta}{\partial x}\right]\right\}-\frac{1}{2}\frac{\partial}{\partial x}\left\{-A_{55}l^2(\frac{\partial\psi_\theta}{\partial x}+\frac{1}{R}\frac{\partial v}{\partial x}-\frac{1}{R}\frac{\partial^2 w}{\partial x\,\partial\theta})\right\}+$$

$$\frac{1}{2R}\frac{\partial}{\partial x}\left\{-B_{55}l^2\left[\frac{1}{R}(\frac{1}{R}\frac{\partial u}{\partial\theta}-\frac{\partial v}{\partial x})+\frac{1}{R}\frac{\partial^2 w}{\partial x\,\partial\theta}-\frac{1}{R}\frac{\partial\psi_x}{\partial\theta}\right]-D_{55}l^2(-\frac{\partial\psi_\theta}{\partial x})\right\}-$$

$$\frac{1}{2}\frac{\partial}{\partial\theta}\left\{-\frac{A_{55}l^2}{2}(\frac{1}{R^2}\frac{\partial v}{\partial\theta}+\frac{\partial^2 w}{\partial x^2}-\frac{1}{R^2}\frac{\partial^2 w}{\partial\theta^2}+\frac{1}{R}\frac{\partial\psi_\theta}{\partial\theta}-\frac{\partial\psi_x}{\partial x})\right\}+ \tag{A.5}$$

$$\frac{1}{2R}\left\{-\frac{A_{55}l^2}{2}\left[-\frac{\partial^2 v}{\partial x^2}-\frac{v}{R^2}+\frac{1}{R}\frac{\partial^2 u}{\partial x\,\partial\theta}+\frac{\psi_\theta}{R}+\frac{1}{R^2}\frac{\partial w}{\partial\theta}\right]-\frac{B_{55}l^2}{2}(\frac{1}{R}\frac{\partial^2\psi_x}{\partial x\,\partial\theta}-\frac{\partial^2\psi_\theta}{\partial x^2})\right\}-$$

$$\frac{1}{2R}\frac{\partial^2}{\partial\theta\,\partial x}\left\{-\frac{B_{55}l^2}{2}\left[\frac{1}{R^2}\frac{\partial^2 u}{\partial\theta^2}-\frac{1}{R}\frac{\partial^2 v}{\partial x\,\partial\theta}+\frac{\psi_x}{R}-\frac{1}{R}\frac{\partial w}{\partial x}\right]-\frac{D_{55}l^2}{2}(\frac{1}{R^2}\frac{\partial^2\psi_x}{\partial\theta^2}-\frac{1}{R}\frac{\partial^2\psi_\theta}{\partial x\,\partial\theta})\right\}-$$

$$\frac{1}{2}\frac{\partial^2}{\partial x^2}\left\{-\frac{B_{55}l^2}{2}\left[-\frac{\partial^2 v}{\partial x^2}-\frac{v}{R^2}+\frac{1}{R}\frac{\partial^2 u}{\partial x\,\partial\theta}+\frac{\psi_\theta}{R}+\frac{1}{R^2}\frac{\partial w}{\partial\theta}\right]-\frac{D_{55}l^2}{2}(\frac{1}{R}\frac{\partial^2\psi_x}{\partial x\,\partial\theta}-\frac{\partial^2\psi_\theta}{\partial x^2})\right\}$$

$$=I_1\left(\frac{\partial^2 v}{\partial t^2}+2(\frac{\partial w}{\partial t})\Omega-v\,\Omega^2\right)+I_2\left(\frac{\partial^2\psi_\theta}{\partial t^2}-\psi_\theta\Omega^2\right)$$

In which parameters used in Eqs. (A.1), (A.2), (A.3), (A.4) and (A.5) are defined as:

$$\{A_{11},B_{11},D_{11}\}=\int_{-\hat{z}_c}^{h-\hat{z}_c}\frac{E(\hat{z},T)}{1-\nu^2(\hat{z},T)}\{1,z,z^2\}dz$$

$$\{A_{12},B_{12},D_{12}\}=\int_{-\hat{z}_c}^{h-\hat{z}_c}\frac{E(\hat{z},T)\nu(\hat{z},T)}{1-\nu^2(\hat{z},T)}\{1,z,z^2\}dz$$

$$\{A_{55},B_{55},D_{55}\}=\int_{-\hat{z}_c}^{h-\hat{z}_c}\frac{E(\hat{z},T)}{2[1+\nu(\hat{z},T)]}\{1,z,z^2\}dz \tag{A.6}$$

$$\{I_0,I_1,I_2\}=\int_{-\hat{z}_c}^{h-\hat{z}_c}\rho(\hat{z},T)\{1,z,z^2\}dz$$

Also, the related boundary conditions are expressed as follows:

$$\delta u = 0 \quad or \quad \int (N_{xx} + \frac{1}{4R}\frac{\partial Y_{xz}}{\partial \theta})d\theta + \int (N_{x\theta} - \frac{Y_{\theta\theta}-Y_{zz}}{2R} + \frac{1}{4}\frac{\partial Y_{xz}}{\partial x} + \frac{1}{2R}\frac{\partial Y_{\theta z}}{\partial \theta})dx = 0,$$

$$\delta u_{,x} = 0 \quad or \quad \int (\frac{\partial Y_{xz}}{4})dx = 0,$$

$$\delta u_{,\theta} = 0 \quad or \quad \int (\frac{\partial Y_{xz}}{4})d\theta + \int (\frac{\partial Y_{\theta z}}{2})dx = 0,$$

$$\delta v = 0 \quad or \quad \int (N_{x\theta} + \frac{Y_{\theta\theta}-Y_{xx}}{2R} - \frac{1}{2}\frac{\partial Y_{xz}}{\partial x} - \frac{1}{4R}\frac{\partial Y_{\theta z}}{\partial \theta})d\theta + \int (N_{\theta\theta} - \frac{1}{4R}\frac{\partial Y_{z\theta}}{\partial x} - \frac{Y_{\theta x}}{2R})dx = 0,$$

$$\delta v_{,x} = 0 \quad or \quad \int (\frac{Y_{zx}}{2})d\theta + \int (\frac{Y_{z\theta}}{4})dx = 0,$$

$$\delta v_{,\theta} = 0 \quad or \quad \int (\frac{Y_{z\theta}}{4})d\theta = 0,$$

$$\delta w = 0 \quad or \quad \int (Q_{xz} + \frac{Y_{z\theta}}{2R} + \frac{1}{2}\frac{\partial Y_{x\theta}}{\partial x} + \frac{1}{4R}\frac{\partial (Y_{\theta\theta}-Y_{xx})}{\partial \theta})d\theta + \int (Q_{\theta z} - \frac{Y_{zx}}{2R} - \frac{1}{2R}\frac{\partial Y_{x\theta}}{\partial \theta} + \frac{1}{4}\frac{\partial (Y_{\theta\theta}-Y_{xx})}{\partial x})dx = 0,$$

$$\delta w_{,x} = 0 \quad or \quad \int (\frac{Y_{x\theta}}{2})d\theta + \int \frac{(Y_{\theta\theta}-Y_{xx})}{4}dx = 0,$$

$$\delta w_{,\theta} = 0 \quad or \quad \int \frac{(Y_{\theta\theta}-Y_{xx})}{4}d\theta + \int (\frac{Y_{x\theta}}{2})dx = 0,$$

$$\delta \psi_x = 0 \quad or \quad \int (M_{xx} + \frac{1}{4R}\frac{\partial P_{xz}}{\partial \theta} + \frac{Y_{x\theta}}{2})d\theta + \int (M_{\theta x} + \frac{1}{4}\frac{\partial P_{xz}}{\partial x} + \frac{1}{2R}\frac{\partial P_{\theta z}}{\partial \theta} + \frac{(Y_{\theta\theta}-Y_{zz})}{2})dx = 0,$$

$$\delta \psi_{x,x} = 0 \quad or \quad \int (\frac{P_{xz}}{4})dx = 0,$$

$$\delta \psi_{x,\theta} = 0 \quad or \quad \int (\frac{P_{xz}}{4})d\theta + \int (\frac{P_{\theta z}}{2})dx = 0,$$

$$\delta \psi_\theta = 0 \quad or \quad \int (M_{x\theta} - \frac{(Y_{xx}-Y_{zz})}{2} - \frac{1}{4R}\frac{\partial P_{\theta z}}{\partial \theta} - \frac{1}{2}\frac{\partial P_{xz}}{\partial x} + \frac{P_{\theta\theta}}{2R})d\theta + \int (M_{\theta\theta} - \frac{Y_{x\theta}}{2} - \frac{1}{4}\frac{\partial P_{\theta z}}{\partial x})dx = 0,$$

$$\delta \psi_{\theta,x} = 0 \quad or \quad \int (\frac{P_{xz}}{2})d\theta + \int (\frac{P_{\theta z}}{4})dx = 0,$$

$$\delta \psi_{\theta,\theta} = 0 \quad or \quad \int (\frac{P_{\theta z}}{4})d\theta = 0$$

(A.7)

Note that the parameters used in Eq. (A.7) are extracted from Eq. (16).

**REFERENCES**

[1]   Ghadiri M., Safarpour H., 2016, Free vibration analysis of embedded magneto-electro-thermo-elastic cylindrical nanoshell based on the modified couple stress theory, *Applied Physics A* **122**: 833.

[2]   Bryan G. H., 1890, On the beats in the vibrations of a revolving cylinder or bell, *Proceedings of the Cambridge Philosophical Society*.

[3]   DiTaranto R., Lessen M., 1964, Coriolis acceleration effect on the vibration of a rotating thin-walled circular cylinder, *Journal of Applied Mechanics* **31**: 700-701.

[4]   Srinivasan A., Lauterbach G. F., 1971, Traveling waves in rotating cylindrical shells, *Journal of Engineering for Industry* **93**: 1229-1232.

[5]   Zohar A., Aboudi J., 1973, The free vibrations of a thin circular finite rotating cylinder, *International Journal of Mechanical Sciences* **15**: 269-278.

[6]   Padovan J., 1973, Natural frequencies of rotating prestressed cylinders, *Journal of Sound and Vibration* **31**: 469-482.

[7]     Padovan J., 1975, Traveling waves vibrations and buckling of rotating anisotropic shells of revolution by finite elements, *International Journal of Solids and Structures* **11**: 1367-1380.

[8]     Padovan J., 1975, Numerical analysis of asymmetric frequency and buckling eigenvalues of prestressed rotating anisotropic shells of revolution, *Computers & Structures* **5**: 145-154.

[9]     Endo M., Hatamura K., Sakata M., Taniguchi O., 1984, Flexural vibration of a thin rotating ring, *Journal of Sound and Vibration* **92**: 261-272.

[10]    Saito T., Endo M., 1986, Vibration of finite length, rotating cylindrical shells, *Journal of Sound and Vibration* **107**: 17-28.

[11]    Huang S., Soedel W., 1988, Effects of coriolis acceleration on the forced vibration of rotating cylindrical shells, *Journal of Applied Mechanics* **55**: 231-233.

[12]    Huang S., Hsu B., 1990, Resonant phenomena of a rotating cylindrical shell subjected to a harmonic moving load, *Journal of Sound and Vibration* **136**: 215-228.

[13]    Yang Z., Nakajima M., Shen Y., Fukuda T., 2011, Nano-gyroscope assembly using carbon nanotube based on nanorobotic manipulation, *Micro-Nano Mechatronics and Human Science (MHS), International Symposium.*

[14]    Malekzadeh P., Heydarpour Y., 2012, Free vibration analysis of rotating functionally graded cylindrical shells in thermal environment, *Composite Structures* **94**: 2971-2981.

[15]    Firouz-Abadi R., Torkaman-Asadi M., Rahmanian M., 2013, Whirling frequencies of thin spinning cylindrical shells surrounded by an elastic foundation, *Acta Mechanica* **224**: 881-892.

[16]    Hosseini-Hashemi S., Ilkhani M., Fadaee M., 2013, Accurate natural frequencies and critical speeds of a rotating functionally graded moderately thick cylindrical shell, *International Journal of Mechanical Sciences* **76**: 9-20.

[17]    Toupin R. A., 1962, Elastic materials with couple-stresses, *Archive for Rational Mechanics and Analysis* **11**: 385-414.

[18]    Koiter W., 1964, Couple stresses in the theory of elasticity, *Proceedings van de Koninklijke Nederlandse Akademie van Wetenschappen.*

[19]    Mindlin R. D., 1964, Micro-structure in linear elasticity, *Archive for Rational Mechanics and Analysis* **16**: 51-78.

[20]    Asghari M., Kahrobaiyan M., Rahaeifard M., Ahmadian M., 2011, Investigation of the size effects in Timoshenko beams based on the couple stress theory, *Archive of Applied Mechanics* **81**: 863-874.

[21]    Yang F., Chong A., Lam D., Tong P., 2002, Couple stress based strain gradient theory for elasticity, *International Journal of Solids and Structures* **39**: 2731-2743.

[22]    Park S., Gao X., 2006, Bernoulli–Euler beam model based on a modified couple stress theory, *Journal of Micromechanics and Microengineering* **16**: 2355.

[23]    Reddy J., 2011, Microstructure-dependent couple stress theories of functionally graded beams, *Journal of the Mechanics and Physics of Solids* **59**: 2382-2399.

[24]    Shaat M., Mahmoud F., Gao X.-L., Faheem A. F., 2014, Size-dependent bending analysis of Kirchhoff nano-plates based on a modified couple-stress theory including surface effects, *International Journal of Mechanical Sciences* **79**: 31-37.

[25]    Ghadiri M., Safarpour H., 2017, Free vibration analysis of size-dependent functionally graded porous cylindrical microshells in thermal environment, *Journal of Thermal Stresses* **40**: 55-71.

[26]    Miandoab E. M., Pishkenari H. N., Yousefi-Koma A., Hoorzad H., 2014, Polysilicon nano-beam model based on modified couple stress and Eringen's nonlocal elasticity theories, *Physica E: Low-dimensional Systems and Nanostructures* **63**: 223-228.

[27]    Love A. E. H., 2013, *A Treatise on the Mathematical Theory of Elasticity* , Cambridge University Press.

[28]    Donnell L. H., 1934, A new theory for the buckling of thin cylinders under axial compression and bending, Transactions of the American Society of Mechanical Engineers **56**: 795-806.

[29]    Sanders Jr J. L., 1959, *An Improved First-Approximation Theory for Thin Shells*, Nasa TR R-24.

[30]    Leissa A. W., 1973, *Vibration of Shells, Scientific and Technical Information Office*, Nasa Report No. SP-288.

[31]    Reissner E., 1945, The effect of transverse shear deformation on the bending of elastic plates, *Journal of Applied Mechanics* **12**: 68-77.

[32]    Mindlin R. D., 1951, Influence of rotary inertia and shear on flexural motions of isotropic elastic plates, *Journal of Applied Mechanics* **18**: 31-38.

[33]    Arani A. G., Zarei M. S., Amir S., Maraghi Z. K., 2013, Nonlinear nonlocal vibration of embedded DWCNT conveying fluid using shell model, *Physica B: Condensed Matter* **410**: 188-196.

[34]    Arani A. G., Kolahchi R., Maraghi Z. K., 2013, Nonlinear vibration and instability of embedded double-walled boron nitride nanotubes based on nonlocal cylindrical shell theory, *Applied Mathematical Modelling* **37**: 7685-7707.

[35]    Hosseini-Hashemi S., Ilkhani M., 2016, Exact solution for free vibrations of spinning nanotube based on nonlocal first order shear deformation shell theory, *Composite Structures* **157**: 1-11.

[36]    Tu Q., Yang Q., Wang H., Li S., 2016, Rotating carbon nanotube membrane filter for water desalination, *Scientific Reports* **6**: 26183.

[37]    Wattanasakulpong N., Ungbhakorn V., 2014, Linear and nonlinear vibration analysis of elastically restrained ends FGM beams with porosities, *Aerospace Science and Technology* **32**: 111-120.

[38]    Safarpour H., Hosseini M., Ghadiri M., 2017, Influence of three-parameter viscoelastic medium on vibration behavior of a cylindrical nonhomogeneous microshell in thermal environment: An exact solution, *Journal of Thermal Stresses* **40**: 1353-1367.

[39]     Barber J. R., 2010, *Intermediate Mechanics of Materials*, Springer Science & Business Media.

[40]     Tauchert T. R., 1974, *Energy Principles in Structural Mechanics*, McGraw-Hill Companies.

[41]     Bellman R., Casti J., 1971, Differential quadrature and long-term integration, *Journal of Mathematical Analysis and Applications* **34**: 235-238.

[42]     Bellman R., Kashef B., Casti J., 1972, Differential quadrature: a technique for the rapid solution of nonlinear partial differential equations, *Journal of Computational Physics* **10**: 40-52.

[43]     Shu C., 2012, *Differential Quadrature and its Application in Engineering*, Springer Science & Business Media.

[44]     Shu C., Richards B. E., 1992, Application of generalized differential quadrature to solve two-dimensional incompressible Navier-Stokes equations, *International Journal for Numerical Methods in Fluids* **15**: 791-798.

[45]     Ghadiri M., Shafiei N., Akbarshahi A., 2016, Influence of thermal and surface effects on vibration behavior of nonlocal rotating Timoshenko nanobeam, *Applied Physics A* **122**: 1-19.

[46]     Beni Y. T., Mehralian F., Razavi H., 2015, Free vibration analysis of size-dependent shear deformable functionally graded cylindrical shell on the basis of modified couple stress theory, *Composite Structures* **120**: 65-78.

[47]     Alibeigloo A., Shaban M., 2013, Free vibration analysis of carbon nanotubes by using three-dimensional theory of elasticity, *Acta Mechanica* **224**: 1415-1427.

[48]     Tadi Beni Y., Mehralian F., Zeighampour H., 2016, The modified couple stress functionally graded cylindrical thin shell formulation, *Mechanics of Advanced Materials and Structures* **23**: 791-801.